Available online at www.sciencedirect.com
SCIENCE DIRECT®
International Journal of Heat and Mass Transfer 48 (2005) 439–453
International Journal of HEAT and MASS TRANSFER
www.elsevier.com/locate/ijhmt

Numerical prediction of flow and heat transfer in a channel in the presence of a built-in circular tube with and without an integral wake splitter

S. Tiwari, D. Chakraborty, G. Biswas *, P.K. Panigrahi

Department of Mechanical Engineering, Indian Institute of Technology Kanpur, Kanpur 208016, India

Abstract

A numerical investigation was carried out to study the heat transfer behavior of a circular tube in cross-flow configuration with a longitudinal fin attached at the rear of the tube. The investigated configuration is intended to model either an element of a cross-flow heat exchanger or an element of the array of pin fins. The longitudinal finning of a circular tube is assumed to be in a configuration where the fin is attached at the back of the circular tube. The longitudinal fins, built-in with the tubes, are called *integral splitter plates*. The splitter plate creates a streamlined extension of the circular tube. It brings about enhancement of heat transfer from the tube surface. A reduction in the size of the wake zone in comparison with the wake of a circular tube is observed. Narrowing of the wake zone reduced convective heat transfer from the tube surface but the splitter plate itself generated an extra fin area for conduction. Overall, there is an improvement in heat transfer past the circular tube with an integral splitter plate compared with the case of flow past a circular tube without a splitter plate. Flow and heat transfer results are presented for three different chord lengths of the splitter plate and three different values of the Reynolds numbers (500, 1000 and 1500). The heat transfer enhancement obtained by finning was compared with that obtained by increasing the diameter of the unfinned tubes.

1. Introduction

Experiments reported by a number of workers [1,2] have shown that the characteristics of the separated wake downstream of obstacles can be greatly influenced if a splitter plate is placed along the centerline of the wake. When a splitter plate is placed downstream of a circular cylinder at the Reynolds numbers at which regular vortices are shed from the cylinder, the vortex shedding may be altered or even suppressed and the drag force experienced by the cylinder may be affected.

Mansingh and Oosthuizen [1] carried out experimental study on the effect of splitter plates on the wake behind a two-dimensional bluff body (a rectangular cylinder) with fixed separation points at low Reynolds numbers (based on the height of the cylinder) between 350 and 1150. Their results indicated that splitter plates alter the pattern of vortex formation in the wake, causing a decrease in shedding frequency, an increase in base pressure and a reduction in overall drag. The effect of splitter plates on the wake flow characteristics of a rectangular cylinder with fixed separation points is similar in nature to that for a circular cylinder with an attached

* Corresponding author. Tel.: +91 0512 597656; fax: +91 0512 597408.
E-mail address: gtm@iitk.ac.in (G. Biswas).

0017-9310/$ - see front matter © 2004 Elsevier Ltd. All rights reserved.
doi:10.1016/j.ijheatmasstransfer.2004.09.003

Nomenclature

C_D	total drag coefficient [$=C_{DF}+C_{DV}$]
C_{DF}	form drag coefficient [$=F_{DF}/\frac{1}{2}\rho U_\infty^2 D$]
C_{DV}	viscous drag coefficient [$=F_{DV}/\frac{1}{2}\rho U_\infty^2 D$]
C_p	coefficient of pressure
D	tube diameter
F_{DF}	form drag
F_{DV}	viscous drag
H	height of the tube
L	chord length of the splitter plate
L_1	axial dimension of the computational domain
L_2	spanwise dimension of the computational domain
l	circumferential length of the tube from the stagnation point
l_c	distance of center of the tube from the inlet
Nu	local Nusselt number
Nu^b_{avg}	Nusselt number, averaged on the bottom wall of channel
Nu^o_{avg}	overall averaged Nusselt number on the tube, splitter plate and the bottom wall
Nu^t_{avg}	Nusselt number, averaged on the tube and the splitter plate surface
Nu_c	local Nusselt number on the tube surface
$\overline{Nu_c}$	height-averaged Nusselt number on the tube surface
$\overline{Nu_s}$	span-averaged Nusselt number on the bottom wall
P	span-averaged pressure
p	static pressure
p_∞	inlet pressure
Q	heat transfer rate
Re_H	Reynolds number based on the channel height, i.e. $\rho U_\infty H/\mu$
Re_D	Reynolds number based on the tube diameter, i.e. $\rho U_\infty D/\mu$
T	temperature
t	time
T_w	wall temperature
T_∞	atmospheric temperature
U_∞	inlet velocity
u_j	velocity vectors
X, Y, Z	non-dimensional coordinates corresponding to x, y and z respectively
x	axial dimension of coordinates
y	spanwise dimension of coordinates
z	normal dimension of coordinates

Greek symbols

α	thermal diffusivity of the fluid
μ	viscosity of the fluid
ρ	density of the fluid
θ	non-dimensional temperature, i.e. $\left(\frac{T-T_\infty}{T_w-T_\infty}\right)$
ϕ	angular location on the tube surface from the forward stagnation point

Subscripts

av	average over the cross-section
b	bulk condition
w	wall

Superscripts

b	bottom wall
o	overall surface area of the tube, splitter plate and the bottom wall
t	tube surface

splitter plate. Anderson and Szewczyk [2] conducted experiments in an atmospheric wind tunnel to study the near wake of a circular cylinder at subcritical Reynolds numbers between 2700 and 46,000. A base-mounted splitter plate was observed to be responsible for the modification of the formation region characteristics without disrupting the usual von Karman shedding. Their results provide an explanation for the non-linearity in the relationship between shedding frequency and the chord length of the splitter plate and extend the findings of the previous investigations of Roshko [3], Gerrard [4] and Apelt et al. [5].

Roshko [3] observed that a splitter plate of chord length *5D,* attached to a circular tube, results in suppression of shedding. Gerrard [4] introduced the concept of *formation length* within which the vortices form before the commencement of shed-ding and a *wake width* at the end of the formation region. He linked the frequency of vortex shedding to these two lengths. Apelt et al. [5] studied the effect of splitter plates on the flow past a circular cylinder in the range $10{,}000 < Re < 50{,}000$. They concluded that the splitter plates reduce the drag significantly by stabilizing the separation points and producing a wake narrower than that for a plane cylinder. The splitter plates raise the base pressure by as much as 50% and affect the Strouhal number to a lesser extent. Sparrow and Kang [6] carried out experimental investigations on longitudinally finned cross-flow tube banks and studied their heat transfer and pressure drop characteristics. They found that a high degree of heat transfer enhancement can be obtained by attaching integral wake splitters at the rear of the tubes. In the terminology of

heat transfer this is called *finning* the tubes. The finning-related enhancements were compared with those attainable with increased diameters of unfinned tubes. Finning was found to be especially advantageous when the comparison is made at fixed pressure drop. They considered finning of the tubes in the tube bundle in various configurations. The fins were attached at both the front and the back of the tube. The experiments were carried out in the Reynolds number (based on tube diameter) range 1000–8600. Patnaik et al. [7] conducted a finite element-based simulation to study the effect of a splitter plate on heat transfer and pressure drop for the case of flow past a circular cylinder at a Reynolds number of 200. Jalaiah [8] demonstrated the contribution of splitter plates to the reduction in drag on circular cylinder flows. In a recent study, Mittal [9] used a *slip* splitter plate in numerical simulations in order to explain the role of the vertical component of momentum in vortex shedding.

A complete numerical analysis of splitter plate-related heat transfer enhancements for moderately high Reynolds numbers has not been accomplished so far. In the present investigation, a numerical study was carried out to determine the flow and heat transfer characteristics for a circular tube with longitudinal fins attached on the rear side. For a given fin length (chord length of the splitter plate), the heat transfer results are presented for various Reynolds numbers. Also for a given Reynolds number, the effect of variation of chord length of the splitter plates on heat transfer was studied.

2. Problem statement

The computational domain for the present problem is shown in Fig. 1. Computations were performed for a circular tube of diameter $D = 4.0H$, H being the height of the domain parallel to the axis of the tube. The domain length along flow direction was $L_1 = 20H$ and the width in the transverse direction $L_2 = 11.25H$. The center of the tube was at a distance $l_c = 6.4H$ from the inlet. For a particular Reynolds number, different chord lengths of the splitter plate were considered for the study of flow structure and heat transfer behavior. Also, for a particular chord length of the splitter plate, computations were performed to investigate the effect of variation of Reynolds number on the behavior of heat transfer. Air was considered as the working fluid, hence the Prandtl number was taken as 0.7. The tube and the splitter plate (longitudinal fin) were considered to be isothermal surfaces.

3. Governing equations

The three-dimensional continuity, Navier-Stokes and energy equations for laminar flow of an incompressible fluid having uniform density are

$$\frac{\partial u_i}{\partial x_i} = 0 \tag{1}$$

$$\frac{\partial u_i}{\partial t} + u_j \frac{\partial u_i}{\partial x_j} = \frac{1}{\rho}\frac{\partial p}{\partial x_i} + \nu \frac{\partial^2 u_i}{\partial x_j \partial x_j} \tag{2}$$

$$\frac{\partial T}{\partial t} + u_j \frac{\partial T}{\partial x_j} = \alpha \frac{\partial^2 T}{\partial x_j \partial x_j} \tag{3}$$

The governing equations are discretized and solved using a Finite Volume algorithm.

4. Boundary conditions

- Top and bottom walls
  These are considered as no-slip walls
  $u = v = w = 0$ and $\frac{\partial p}{\partial z} = 0$
  $T = T_w$
  (T_w represents wall temperature)

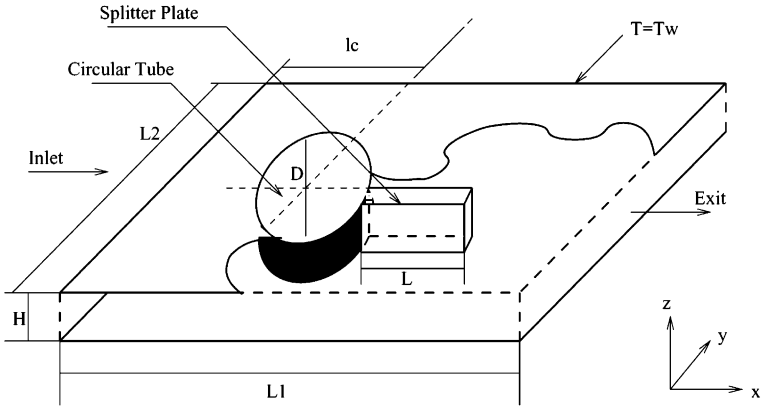

Fig. 1. Three-dimensional computational domain describing the channel with built-in circular tube and the splitter plate.

- Side walls
  $\frac{\partial u}{\partial y} = \frac{\partial w}{\partial y} = v = 0$
  (free-slip boundary condition) and
  $\frac{\partial p}{\partial y} = 0,\ \frac{\partial T}{\partial y} = 0$
- Channel inlet
  $u = U_\infty$; $v = w = 0$ and $\frac{\partial p}{\partial x} = 0$;
  $T = T_\infty$
- Channel exit
  The mass flux through the outlet boundaries is found by means of a convective outflow condition, according to Orlanski [10], which allows changes inside the flow field to be transmitted outward, but not vice versa. This boundary condition uses an upwind form of the following equation for each velocity component and temperature.
  $\frac{\partial \phi}{\partial t} + U_{\text{av}} \frac{\partial \phi}{\partial x} = 0$
  (where ϕ represents u, v, w or T)
  The pressure is also specified at the outflow:
  $p = p_\infty$
- Obstacles (surface of the circular tube and the splitter plate)
  $u = v = w = 0$; $\frac{\partial p}{\partial n} = 0$
  (where n signifies the normal direction to the surface) and $T = T_{\text{w}}$ ($T_{\text{w}} > T_\infty$)

5. Grid generation

Fig. 2 shows a schematic representation of the two-dimensional grid employed in the present computation. The two-dimensional grid of body-fitting type is generated using the method of transfinite interpolation. It is further improved with the help of the partial differential equations technique [11]. In order to generate the three-dimensional grid, the two-dimensional grids on the x–y plane are stacked in the z-direction with constant Δz.

6. Solution algorithm

A finite-volume method due to Eswaran and Prakash [12] was used to discretize and solve the governing conservation equations. The pressure-velocity iterations follow the method due to Harlow and Welch [13]. The numerical procedure of Eswaran and Prakash [12] was documented in the work of Prabhakar et al. [14]. The method has been successfully applied to related problems [11,15].

7. Result and discussion

A $61 \times 49 \times 21$ grid is used for the case of a tube with a splitter plate. A grid-independence study was conducted and the grid size of $61 \times 49 \times 21$ was able to produce a grid-independent solution. Computations were carried out for three different chord lengths of the splitter plate ($L = 2H$, $3H$ and $4H$) and three different Reynolds numbers (500, 1000 and 1500). The chord length of the splitter plate for all other parametric variations is considered to be $L = 2H$ except for the cases where the comparison of heat transfer performance is made for different chord lengths of the splitter plate. The divergence-free criterion is satisfied using an upper bound of 10^{-4}. Local and average Nusselt numbers are calculated on the basis of bulk-mean temperature.

7.1. Flow characteristics

The use of splitter plates to add surface area can bring about a substantial increase in the heat transfer from the tube. The presence of the splitter plate also influences the pressure drop characteristics of the tube.

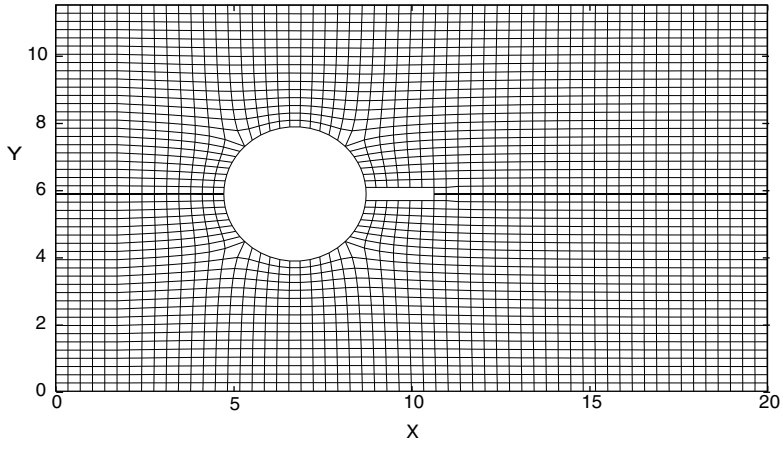

Fig. 2. Schematic of the grid system on the x–y plane.

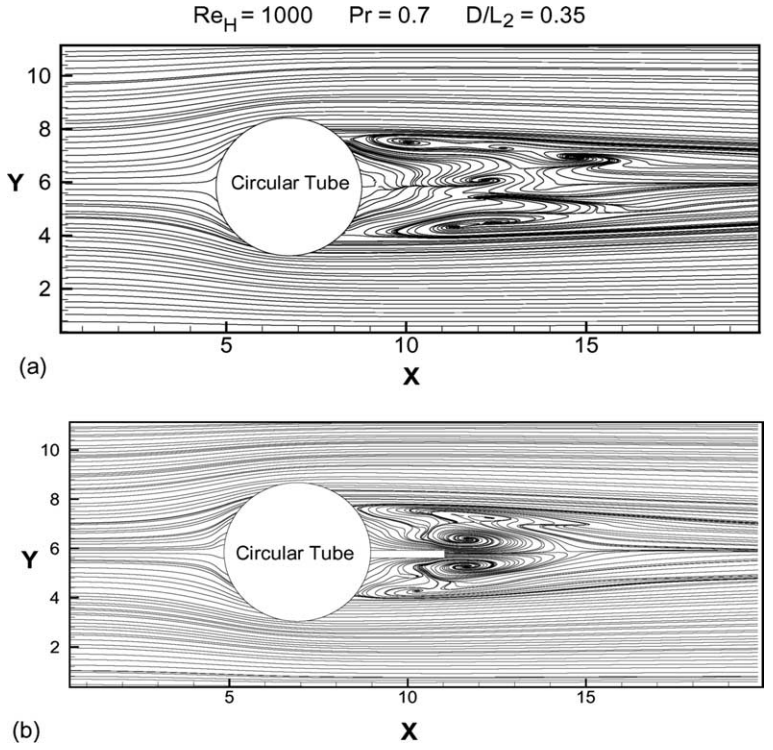

Fig. 3. Streamline plots of the instantaneous field at the horizontal midplane of the channel for the case of flow past (a) circular tube and (b) circular tube with splitter plate of chord length $L = 2H$.

Fig. 3 shows the streamline paths of an instantaneous flow field at the horizontal midplane for flow past a circular tube and the circular tube with an integral splitter plate. In Fig. 3(a), the flow past a circular tube displays vortex shedding, as evident from the asymmetry observed in the wake structure. It has already been established in the literature that the vortex shedding for flow past a circular tube, placed in an infinite medium, begins at a low Reynolds number ($Re \simeq 50$). The Reynolds number in the present study ($Re_H = 1000$, $Re_D = 4000$) is fairly large and alternate shedding of vortices is a ubiquity. The wake splitter has frequently been used as a passive means of controlling vortex formation and shedding in the near wake of a circular tube. The flow field at the horizontal midplane for the case of flow past a circular tube with integral splitter plate (Fig. 3(b)) illustrates a symmetric behavior even though it is an instantaneous flow field. For a plain circular tube (without a splitter plate), the shear layers exhibit transverse oscillations in-phase with the von Kármán shedding cycle. The attachment of even a very short splitter plate is sufficient to diminish the amplitude of the oscillations. The splitter plates prevent the interaction of the separated shear layers on either side of the plate surface. For certain combinations of blockage ratios, chord lengths of the plate and Reynolds numbers, even the shedding can be completely eliminated.

Fig. 4 shows the streamlines on the horizontal midplane of the channel for two different chord lengths of the splitter plate ($L = 3H$ and $L = 4H$). In both cases the flow fields illustrate a good degree of symmetry even though the flow fields are unsteady.

A plain circular tube has its vortex formation region as shown in Fig. 3(a). The splitter plate of chord length $2H$ causes the vortex to form clear off the plate as in Fig. 3(b). As the chord length of the plate increases, vortices move towards the plate and roll over the edge as in Fig. 4. The position of vortex formation does not alter significantly downstream as L increases from $2H$ to $4H$. Beyond $L = 3H$, the formation position remains essentially at the same location with respect to the circular tube. The formation region for $L = 4H$ is slightly downstream as compared with all the other cases.

Fig. 5 shows the limiting streamline plots of the instantaneous field in the region close to the bottom wall of the channel for the case of a built-in plain circular tube and the case of a built-in circular tube with a splitter plate of chord length = $2H$ for a Reynolds number, $Re_H = 1000$. Fig. 5(a) and (b) show the streamline plots

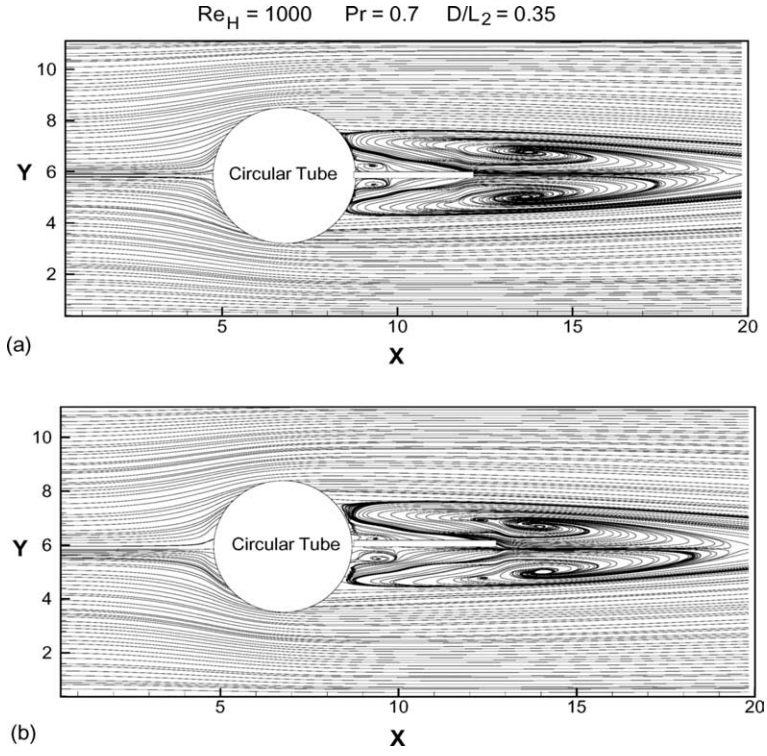

Fig. 4. Steady-state streamlines on the horizontal midplane of the channel for the case of a built-in circular tube with splitter plate of chord length (a) $L = 3H$ and (b) $L = 4H$.

very close to the bottom wall of the channel at a normal distance of $Z = 0.06H$ from the wall. The two plots are similar except in the region where the splitter plate is attached. In a similar way, Fig. 5(c) and (d) are at a normal distance of $Z = 0.12H$ from the bottom wall, and Fig. 5(e) and (f) are at a normal distance of $Z = 0.18H$ from the wall. In Fig. 5(a) and (b), a saddle point of separation and a horseshoe vortex system are observed. The incoming flow reaches a stagnation or saddle point of separation and goes around the body. The nodal point of attachment and the separation lines which form circular arcs across the tube can be seen. The flow above the bottom wall hits the front of the tube. A significant part of it moves downwards and creates a region of reversed flow in front of the stagnation line. On each side of the tube, there is a region of converging streamlines. These are the traces of horseshoe vortices. The mean shear within the approaching boundary layer is skewed or deflected by the transverse pressure gradient. Accordingly, the boundary layer separates and rolls up to form a spanwise vortex. The horseshoe vortex system has a strong influence on the overall convective heat transfer. The flow past the circular tube alone in the absence of a splitter plate (Fig. 5(a), (c) and (e)) displays asymmetry in the wake zone. In presence of the splitter plate, the flow field in the wake zone displays nearly symmetrical behavior about the longitudinal vertical midplane (Fig. 5(b), (d) and (f)). With attachment of the splitter plate, the flow becomes more streamlined and the flow field closely resembles a steady-state flow field. In this case, a wake stagnation point further downstream in the wake zone is observed which is not present in the case of a circular tube without the splitter plate.

The structure of the surface streamlines or limiting streamlines on the surfaces of both circular tube and splitter plate was investigated. These streamlines consist of only tangential components of velocity near the surfaces of the tube and the splitter plate. Fig. 6 shows such streamlines. The time-averaged flow field is symmetric and the limiting streamlines are symmetrically distributed about the midplane of the channel. The surface streamlines reveal bifurcation. The bifurcation could be either a positive bifurcation or a negative bifurcation. When one streamline divides into two or more streamlines, it is called a positive bifurcation. If two or more streamlines combine to form a single streamline, it is called a negative bifurcation. Fig. 6 reveals the positive bifurcation at the forward stagnation line of the tube surface ($\theta = 0$ or $\theta = 2\pi$). It is also observed from Fig. 6 that for a plain circular tube the line of reattachment is at $\theta = \pi$ and for the splitter plate it is at the tip of the plate. As the chord length of the splitter plate in-

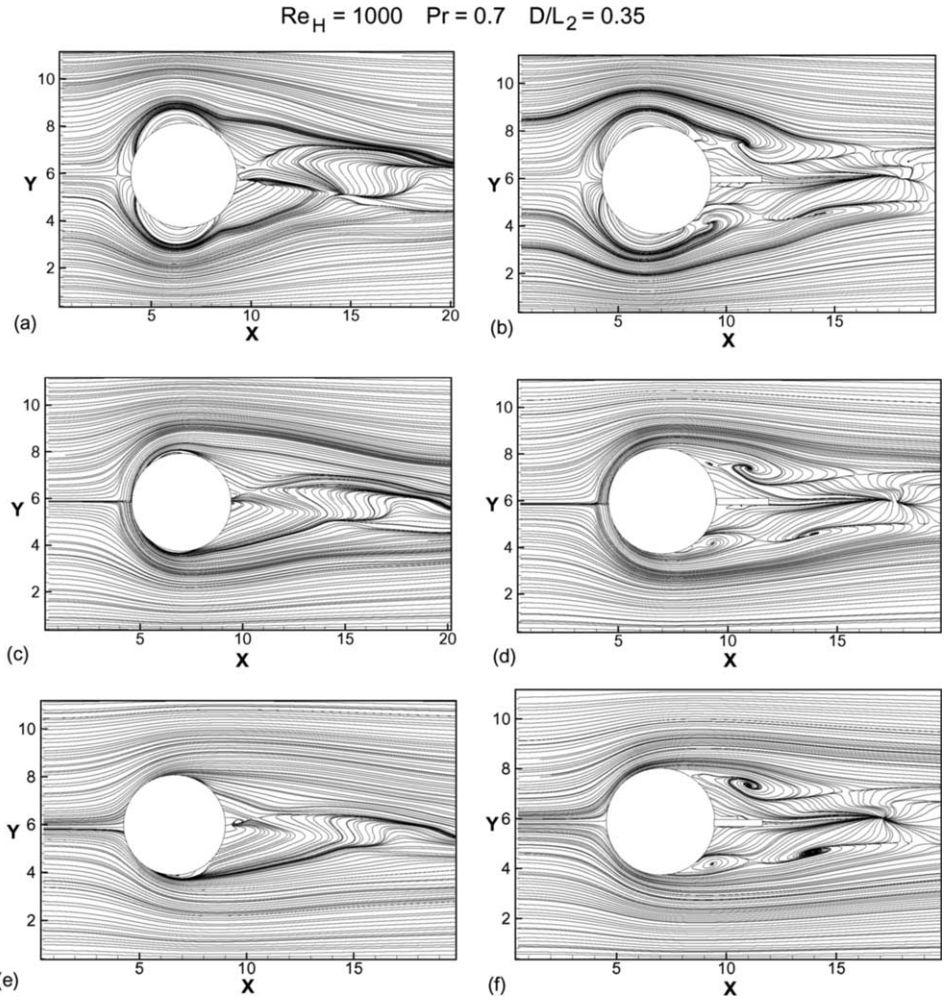

Fig. 5. Instantaneous streamlines very near the bottom wall of the channel at different normal distances, (a), (c) and (e) are for a circular tube and (b), (d) and (f) are for circular tube with splitter plate of chord length $L = 2H$, at normal distances $z = 0.06H$, $0.12H$ and $0.18H$ respectively.

creases, the streamlines on either side of the line of reattachment are straightened. Fig. 6(a) shows two other lines at $0.61\pi < \theta < 0.81\pi$ and $1.19\pi < \theta < 1.39\pi$. Near these lines, the tangential components of the shear stress vectors vanish. Hornung and Perry [16] called this a negative stream surface bifurcation. These lines can be termed separation lines, along which the boundary layer separates from the tube surface. The separation angles (on the tube surface) for the cases with splitter plates (of varying chord lengths) remain almost same as compared with the separation angles for the case without a splitter plate. However, this is not directly evident from Fig. 6 since the chord lengths ofthe splitter plates have been added to the scales for the abscissa. A closer observation reveals that the presence of splitter plates delays the flow separation.

7.2. Temperature distribution

Fig. 7(a) shows the temperature distribution of the cold fluid at locations close to the tube surface for the plain circular tube. Fig. 7(b) shows the same for the case of a circular tube with a splitter plate of chord length $2H$. Fig. 7(a) reveals that the minimum temperature of the fluid is at the forward stagnation line of the tube. The temperature increases as the flow moves towards the point of reattachment. The incoming cooler fluid strikes the stagnation line and removes heat from the stagnation region. After striking the tube, the fluid gains some thermal energy and the energy in the fluid increases by taking heat from the tube surface by convection as it progresses embracing the tube surface. This figure also shows that the temperature is higher near

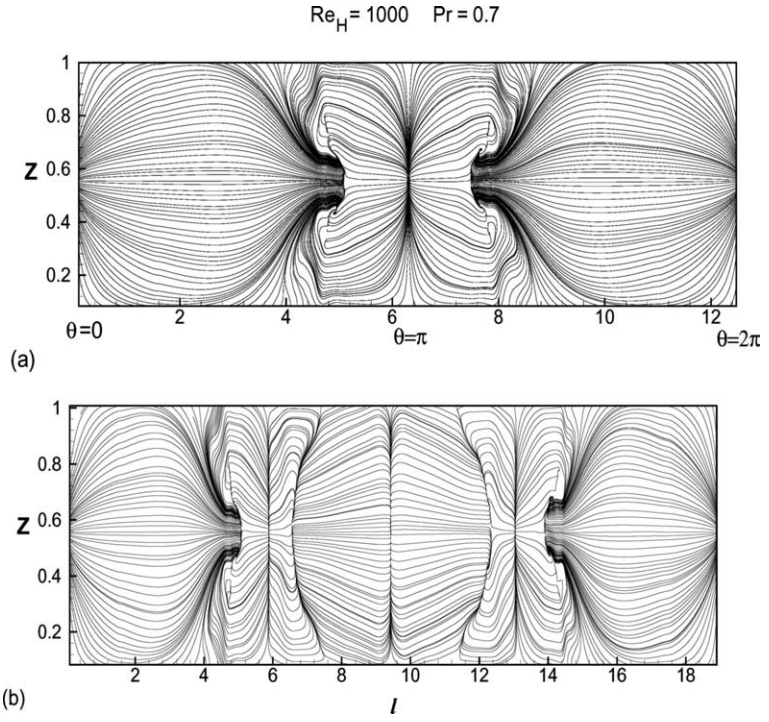

Fig. 6. Limiting time-averaged streamlines on the surface of the (a) circular tube and (b) circular tube with splitter plate of $L = 2H$.

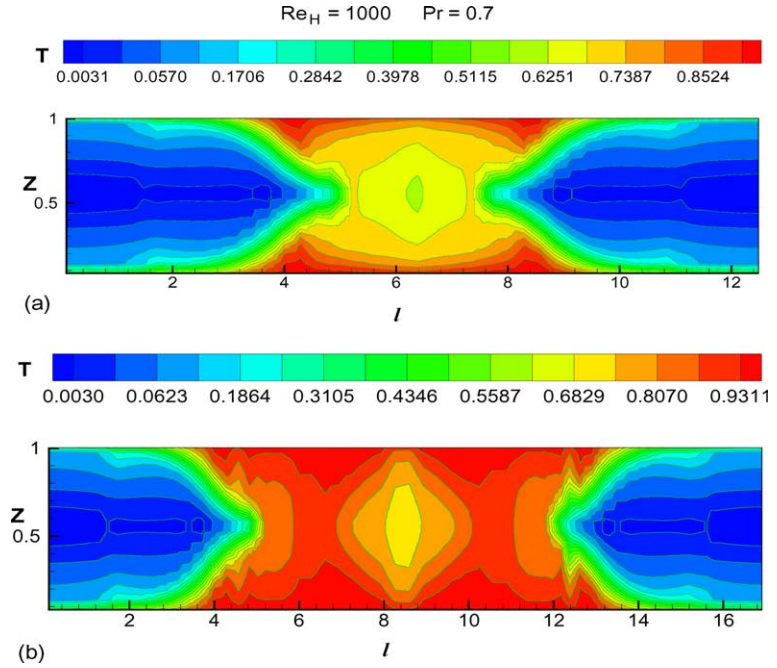

Fig. 7. Temperature distribution of the cold fluid layer close to the surface of (a) circular tube and (b) circular tube with splitter plate of chord length $L = 2H$.

the bottom and top walls as compared with the middle portion of the channel. At the splitter plate part, it is observed that as the fluid progresses towards the tip of the plate, its temperature decreases from the maximum value even though the temperature remains fairly high. In Fig. 7(a) and (b), the circular tube and the circular tube with the splitter plate of chord length $2H$ retain symmetry in the distribution of the temperature field with respect to the plane $z = H/2$. The reason could be attributed to the influence of the splitter plate in streamlining the flow.

7.3. Nusselt number distribution

The local Nusselt number on the bottom wall may be defined as

$$Nu = \left(\frac{\partial\theta}{\partial Z}\right)_{\text{wall}} \tag{4}$$

Fig. 8 shows the contour map of the iso-Nusselt number on the bottom wall. Before starting the discussion of this plot, there are some issues which should be addressed. In a realistic situation, the tube wall and the splitter plate (longitudinal fin) do not possess constant temperature because both convective and conductive heat transfer take place from the tube wall and the fin surface. However, in the present computation, it is assumed that the tube wall and the longitudinal fin are at constant temperature. Fig. 8 depicts that at the leading edge of the bottom wall, the Nusselt number has its maximum value and it decreases gradually until some specified position before the tube. At the leading edge, the cooler fluid comes in contact with the hot solid wall for the first time, hence the temperature gradient becomes maximum, entailing a very high value of the Nusselt number. The inlet condition is one of uniform velocity in addition to uniform inlet temperature. Therefore, both the velocity and thermal boundary layers develop at the channel leading edge. The region that follows the leading edge of the channel is the combined entrance region. There is a sudden increase in Nusselt number in front of the tube. The reason for the abrupt increase in Nusselt number can be attributed to the formation of horseshoe vortices. The spiraling motion of the horseshoe vortices brings about better mixing and the heat transfer in this region is enhanced significantly. The Nusselt number is low in the wake region. The separated dead water zone where fluid recirculates

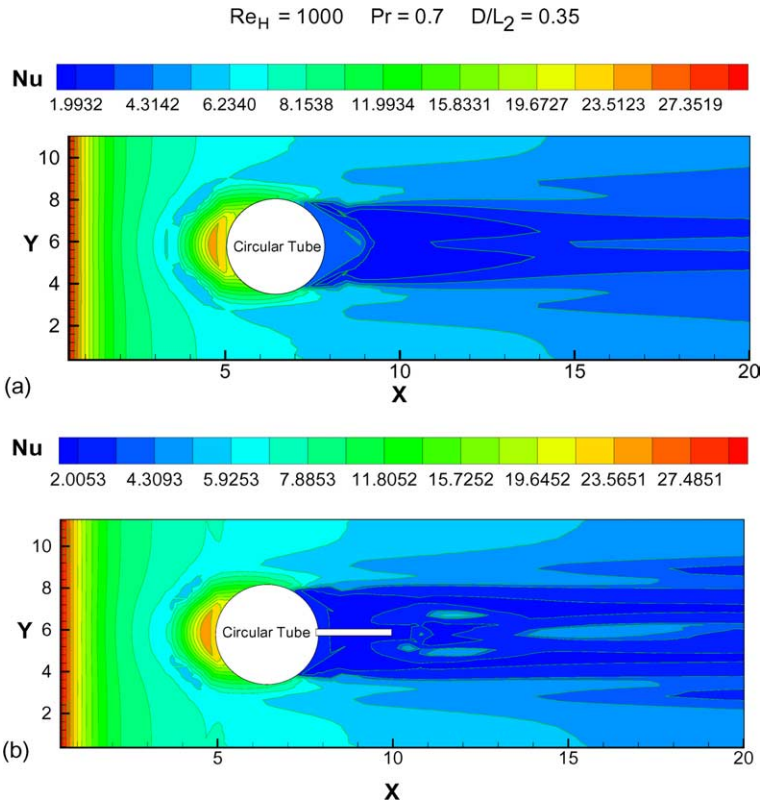

Fig. 8. Iso-Nusselt number distribution at the bottom wall for the cases of a channel with a built-in (a) circular tube and (b) circular tube and a splitter plate of chord Length $L = 2H$.

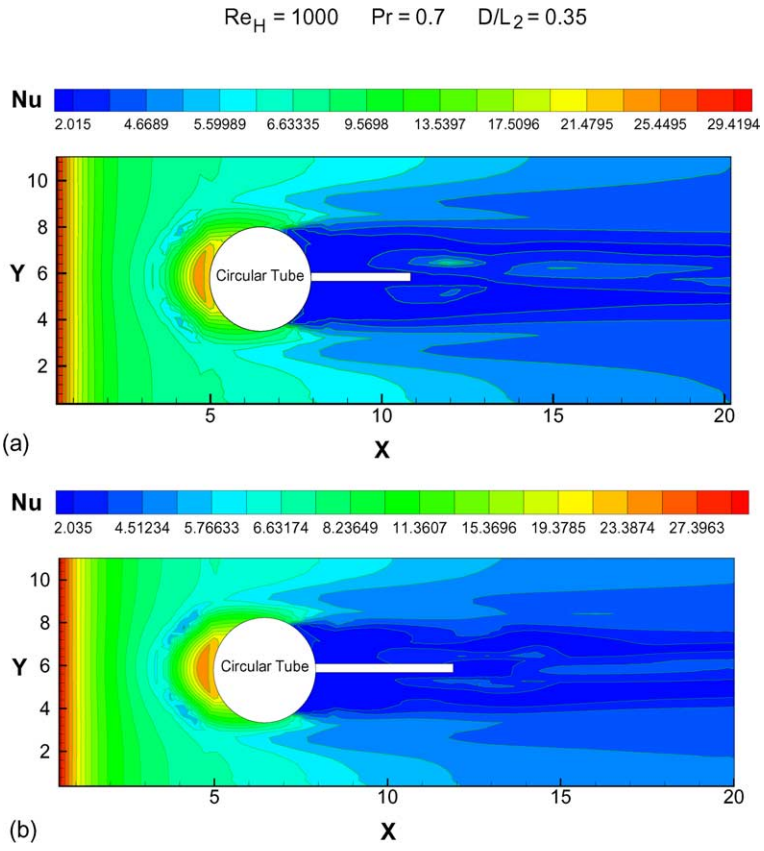

Fig. 9. Iso-Nusselt number distribution at the bottom wall for the cases of a channel with a built-in circular tube and a splitter plate of chord length (a) $L = 3H$ and (b) $L = 4H$.

with low velocity causes poor heat transfer. Figs. 8(b) and 9(a) and (b) show the contour plots of iso-Nusselt number distribution on the bottom wall for splitter plates of varying chord length ($L = 2H$, $3H$ and $4H$). The Nusselt number distribution pattern from the leading edge of the channel to the location of the tube in all cases is similar to that of the channel with a built-in plain circular tube. The heat transfer enhancement due to the attachment of the splitter plate is evident in the zone near the location of the tip of the splitter plate. As the chord length of the splitter plate increases, the size of the zone of high heat transfer in the wake increases.

The presence of a splitter plate causes a general decrease in the local heat transferrate over the surface of the circular tube. The local Nusselt number on the tube surface and the splitter plate may be defined as

$$Nu_c = \left(\frac{\partial\theta}{\partial n}\right)_{\text{surface}} \tag{5}$$

where n is along normal to the surface of the tube or splitter plate.

A decrease in local heat transfer occurs because the interaction of the vortices on either side of the splitter plate ceases. However, the splitter plate provides an additional heat transfer surface and overall heat transfer is enhanced. A parameter could be formulated to estimate the gain in heat transfer due to the splitter plate in the following way

$$Nu^{t}_{\text{avg}} = \frac{\int_{A_0} Nu_c \cdot dA + \int_{A-A_0} Nu_c \cdot dA}{A} \tag{6}$$

where A_0 is the surface area of the tube and A is the combined surface area of the tube and the splitter plate.

The Nusselt number averaged over tube and splitter plate surface (Nu^{t}_{avg}) for different chord lengths of the splitter plate is calculated for three different Reynolds numbers, $Re_H = 500$, 1000 and 1500. The Q/Q_0 ratios deduced from these Nusselt numbers are shown in Table 1. The pertinent parameters in Table 1 are L, A/A_0 and Q/Q_0; Q is the heat transfer from the combined surface area of the splitter plate and the circular tube and Q_0 is the heat transfer from the circular tube alone. It is clear from Table 1 that $Q/Q_0 > 1$ when $A/A_Q > 1$. For the case when $A/A_0 = 1.60$, Q/Q_0 could be compared with the results of Sparrow and Rang [1]. In our computation we observe $Q/Q_0 = 1.369$, which is lower than the

Table 1
Values of Q/Q_0 for the splitter plates of three different chord lengths

Reynolds number (Re_H)	Chord length (L)	A/A_0	Q/Q_0
500	$2H$	1.32	1.09
	$3H$	1.48	1.18
	$4H$	1.63	1.28
1000	$2H$	1.32	1.20
	$3H$	1.18	1.29
	$4H$	1.63	1.40
1500	$2H$	1.32	1.38
	$3H$	1.48	1.49
	$4H$	1.63	1.61

result of Sparrow and Kang [1] by 7%. The reason could be the following. The tube length in their experiments was fairly long so that a nominally two-dimensional situation evolved and the transport mechanism was free from the influence of top and the bottom walls. In the present computation, the top and the bottom walls play a significant role. The gap between the top and the bottom walls *is* fairly small and the length of the tube is restricted by the gap.

Table 2 shows the variation of Nu^t_{avg} with Reynolds number. As the Reynolds number increases, Nu^t_{avg} also increases. An increase in Reynolds number means increase in inlet velocity. It is understood that the splitter plate is more effective at higher Reynolds numbers.

The splitter plate creates a streamlined extension of the circular tube, which also brings about enhancement of heat transfer. A reduction in the size of wake zone is observed. Narrowing of the wake zone reduces convective heat transfer from the tube surface but the splitter plate itself generates an extra fin area for conduction. Overall, there is an improvement in heat transfer past

Table 2
Variation of Nu^t_{avg} with Reynolds number for a splitter plate of chord length = $2H$

Reynolds number (Re_H)	Nu^t_{avg}	Q/Q_o
500	4.54	1.09
1000	5.23	1.20
1500	6.04	1.38

the circular tube with an integral splitter plate compared with the case of flow past a plain circular tube. The heat transfer enhancement obtained by finning in this way can be compared with that which could be obtained by increasing the diameter of unfinned tubes. The computation was carried out for equal heat transfer surface area of unfinned tube having increased diameter and finned tube at a particular Reynolds number of $Re_D = 4000$. The area ratio considered to investigate the performance of the finned tube is $A/A_0 = 1.32$. At the area ratio of 1.32 and for $Re_D = 4000$, the value of Nu^t_{avg} is 5.23 for the case of a circular tube with a splitter plate of chord length $2H$ and the value of Nu^t_{avg} is 4.88 for the case of a plain circular tube of increased diameter. Hence finning gives a better result for heat transfer compared with the increased diameter circular tube.

Fig. 10 shows a comparison of height-averaged Nusselt number distribution ($\overline{Nu}_c$) on the tube and splitter plate surface for different chord lengths. The presence of the splitter plate causes a general decrease in the local heat transfer rate over the whole surface of the circular tube. The effect is more pronounced over the wake region and is stronger for length $2H$. The decrease in local heat transfer can be attributed to the absence of interaction of the vortices on either side of the splitter plate and the relative decrease in mixing of vortices with the outer layers of the flow. Fluctuations in the Nu_c distribution

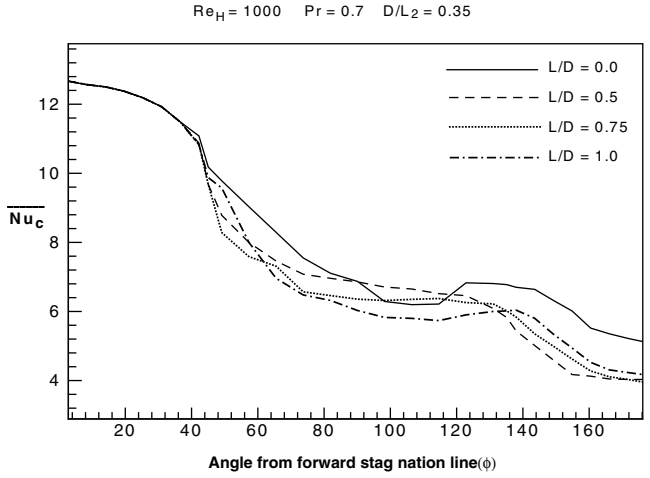

Fig. 10. Height-averaged Nusselt number distribution on the surface of circular tube for different chord lengths of the splitter plate.

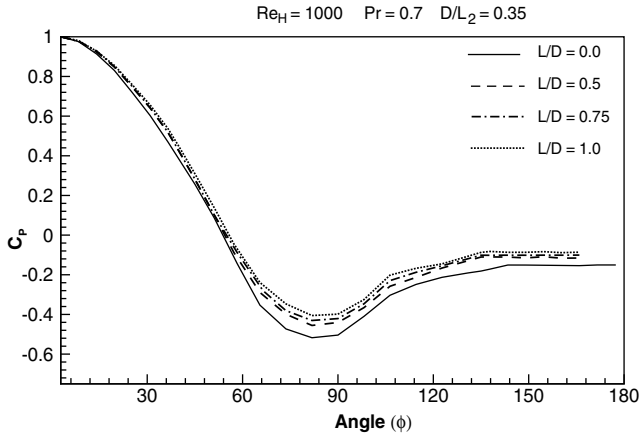

Fig. 11. Comparison of distribution of C_p around the tube surface for four different splitter plate chord lengths ($L = 0$, $2H$, $3H$ and $4H$).

over the wake region of the circular tube and on the splitter plate surface can be attributed to the separated and reattached boundary layer enclosing a region of reverse flow between the surfaces of the plate and the circular tube.

Fig. 11 shows the distribution of pressure coefficient $C_p = \frac{p-p_\infty}{p_s-p_\infty}$, where p is the local pressure, p_s is the stagnation pressure and p_∞ is the atmospheric pressure for the case of a circular tube in uniform flow with splitter plate of different chord lengths at $Re_H = 1000$. The profiles indicate that the pressure in the separated region, adjacent to the circular tube, is sensitive to the variations in chord length of the splitter plate. The pressure variation agrees well with the trends of variation in the earlier work of Apelt et al. [5]. The reason for an increase in the base pressure clue to presence of the splitter plate appears to be as follows. It was mentioned earlier that the splitter plate delays the flow separation slightly. However, this delay in separation does not cause any significant effect in the wake zone. The small rise in base pressure is expected to decrease the total drag. The coefficient of total drag, C_D, can be written as $C_D = C_{DF} + C_{DV}$ with the form drag and viscous drag represented as

$$C_{DF} = \frac{F_{DF}}{\frac{1}{2}\rho U_\infty^2 D} \quad \text{and} \quad C_{DV} = \frac{F_{DV}}{\frac{1}{2}\rho U_\infty^2 D} \tag{7}$$

where F_{DF} and F_{DV} are the form drag and the viscous drag forces obtained by integrating pressure and viscous shear forces over the surfaces of the cylinder and the splitter plate, respectively. The results pertaining to the drag coefficients are shown in Table 3. One would expect the value of C_{DV} to increase with increasing chord length of the splitter plate. However, the counter rotating vortices (see Fig. 4) diminish the effect of viscous drag on the chord of the splitter plate.

Table 3
Variation of C_D, C_{DF} and C_{DV} with the chord length of the splitter plate for $Re_H = 1000$

Chord length	C_{DF}	C_{DV}	C_D
0	1.234	0.0453	1.2793
$2H$	0.9911	0.0433	1.0344
$3H$	0.9856	0.0423	1.0279
$4H$	0.983	0.0411	1.0241

It can also be seen from Table 3 that, with increase in chord length of the splitter plate, the values of C_{DF} and C_D decrease marginally. The values of C_{DV} are very small in all cases.

Fig. 12 shows the distribution of span-averaged Nusselt number ($\overline{Nu_s}$) along the length of the channel for the circular tube without splitter plate and circular tube with an integral splitter plate with three different chord lengths. It is observed that the effect of variation of the span-averaged Nusselt number shows no difference for these cases from the inlet until the vicinity of the forward stagnation line of the circular tube. This is due to almost identical nature of the flow field for these cases. In the downstream region, the span-averaged Nusselt number is observed to increase with increase in the length of the splitter plate. This increase is due to the combined heat transfer by convection and conduction showing an enhancement in the energy transport. The increase in span-averaged Nusselt number is observed to be more effective in the wake zone and is of the order of 10–20%. This increase in span-averaged Nusselt number and the reduction in pressure penalty (Fig. 11) offer a positive recommendation for use of splitter plates in fin-tube heat exchangers.

Fig. 13 shows the distribution of span-averaged pressure (P) along the length of the channel for a circular

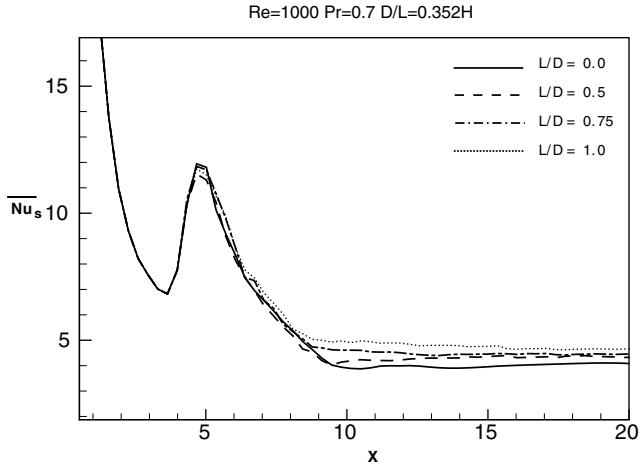

Fig. 12. Comparison of span-averaged Nusselt number distribution for different chord lengths of splitter plate and of circular tube with no splitter plate.

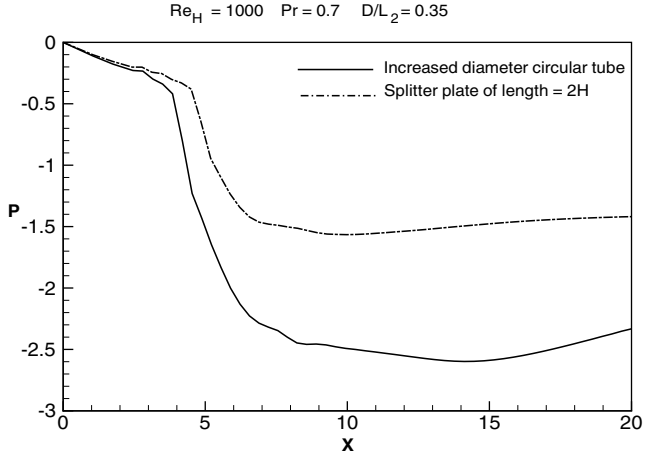

Fig. 13. Comparison of span-averaged pressure distribution for splitter plate of chord length $L = 2H$ with circular tube of increased diameter.

tube with a splitter plate of chord length $2H$ and a circular tube of increased diameter having a perimeter equal to the circular tube and the splitter plate. This comparison between finned and unfinned tubes of same surface area is presented for a fixed value of the Reynolds number ($Re_D = 4000$). It can be seen that the pressure penalty is high in the unfinned circular tube of increased diameter compared with the finned tube. That is because the increased diameter circular tube provides a greater blockage to the flow.

Figs. 11 and 12 together indicate that finning of the circular tube improves heat transfer and reduces the pressure penalty. As a consequence, it could be recommended as a good modification to the circular tubes employed in fin-tube heat exchangers. The averaged Nusselt number on the tube and splitter plate surface (Nu^{t}_{avg}) was computed for different chord lengths of the splitter plate. Also, the averaged Nusselt number at the bottom wall (Nu^{b}_{avg}) was calculated for the same varying geometric parameters. Table 4 shows the variation of tube surface-based averaged Nusselt number and the

Table 4
Variation Nu^{t}_{avg}, Nu^{b}_{avg} and Nu^{o}_{avg} with the chord length of the splitter plate for $Re_H = 1000$

Chord length	Nu^{t}_{avg}	Nu^{b}_{avg}	Nu^{o}_{avg}
0	5.87	6.48	6.44
$2H$	5.65	6.42	6.35
$3H$	5.58	6.44	6.36
$4H$	5.63	6.46	6.38

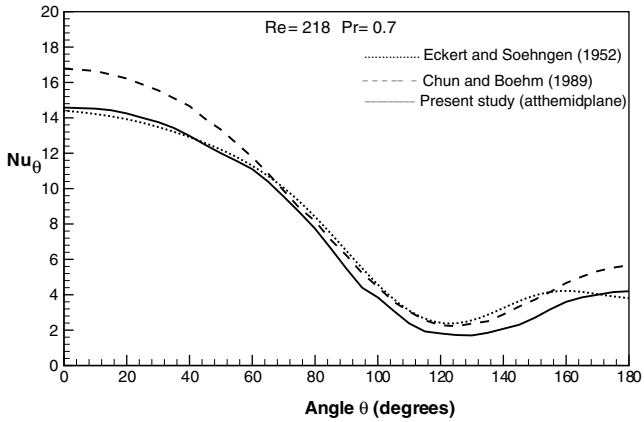

Fig. 14. Comparison of local Nusselt number distribution on the tube surface.

averaged Nusselt number on the bottom wall for different chord lengths of the splitter plate. The overall Nusselt number for the total surface area (combined surface area of the tube with splitter plate and the channel walls) (Nu^{o}_{avg}) was also calculated and is shown in Table 4.

Fig. 10 and Table 4 demonstrate that as the chord length of the splitter plate increases, the averaged Nusselt number, near the tube surface, first decreases and then increases. They also reveal that the increase in the global Nusselt number at the bottom wall is quite small with the increase in the chord length of the splitter plate. The variation in the overall Nusselt number is also fairly small for different chord lengths of the splitter plate. The surface area of the tube is fairly small compared with the surface area of the bottom (or top) walls and so the variation of the overall Nusselt number is similar to the variation of the Nusselt number at the bottom wall. The model validation was performed through comparison with the experimental results of Eckert and Soehngen [17] and numerical results of Chun and Boehm [18] for a Reynolds number of 218 for the case of flow past a circular tube without any wake splitter. Fig. 14 shows the comparison of local Nusselt numbers along the circumference of the tube at the horizontal midplane. The present computation compares favorably with the experiments of Bckert and Soehngen [17].

8. Conclusions

Particular attention has been paid to the study of the variation of the coefficient of pressure, coefficient of drag, vortex structure, limiting streamlines and heat transfer with the chord length of the splitter plate. This study has shown that the characteristics of the wake downstream of a circular tube can be altered by placing a splitter plate on the wake centerline downstream of the circular tube. Flow visualization indicated that a splitter plate produced a stabilizing effect via reduction of transverse 'flapping' of the shear layers. The splitter plate streamlines the flow. The vortices are pushed downstream, followed by narrowing of the wake. Usually, the plate does not inhibit the formation of vortices, but the vortical motion does not extend far downstream. The heat transfer is decreased from the tube surface. However, the presence of the splitter plate increases the total heat transfer substantially by complementing for extended surface heat transfer. Hence, the splitter plate results in an overall enhancement of heat transfer. The splitter plate being a slender body reduces the pressure loss penalty significantly.

Acknowledgment

This investigation was sponsored by the New Energy and Industrial Development Organization (NEDO), Japan.

References

[1] V. Mansingh, P.H. Oosthuizen, Effects of splitter plates on the wake flow behind a bluff body, A1AA J. 28 (1990) 778–783.
[2] E.A. Anderson, A.A. Szewczyk, Effects of a splitter plate on the near wake of a circular cylinder in 2 and 3-dimensional flow configurations, Exp. Fluids 23 (1997) 161–174.
[3] A. Roshko, On the drag and shedding frequency of two-dimensional bluff bodies, Technical Report TN 3169, NACA, 1954.
[4] J.H. Gerrard, The mechanics of the formation region of vortices behind bluff bodies, J. Fluid Mech. 25 (1966) 401–413.
[5] C.J. Apelt, G.S. West, A.A. Szewczyk, The effects of wake splitter plates on the flow past a circular cylinder in the

range of 10,000 <Re < 50,000., J. Fluid. Mech. 61 (1973) 187–198.
[6] E.M. Sparrow, S.S. Kang, Longitudinally-finned cross-flow tube banks and their heat transfer and pressure drop characteristics, Int. J. Heat Mass Transfer 28 (1985) 339–350.
[7] B.S.V.P. Patnaik, K.N. Seetharamu, P.A. Aswatha Narayana, Simulation of laminar confined flow past, a circular cylinder with integral wake splitter involving heat transfer, Int. J. Numer. Methods Heat Fluid Flow 6 (1996) 65–81.
[8] N. Jalaiah, Numerical simulation on confined flow past a circular cylinder with integral wake splitter, Ph.D. thesis, Indian Institute of Technology Madras, 2001.
[9] S. Mittal, Effect of a slip splitter plate on vortex shedding from a cylinder, Phys. Fluids 15 (2003) 817–820.
[10] I. Orlanski, A simple boundary condition for unbounded flows, J. Comput. Phys. 21 (1976) 251–269.
[11] S. Tiwari, D. Maurya, G. Biswas, V. Eswaran, Heat transfer enhancement incross flow heat exchangers using oval tubes and multiple delta winglets, Int. J. Heat Mass Transfer 46 (2003) 2841–2856.
[12] V. Eswaran, S. Prakash, A finite volume method for Navier–Stokes equations, in: Proceedings of the Third Asian CFD Conference, Bangalore, vol. 1, 1998, pp. 127–133.
[13] F.H. Harlow, W.E. Welch, Numerical calculation of time-dependent viscous incompressible flow of fluid with free surface, Phys. Fluids 8 (1965) 2182–2188.
[14] V. Prabhakar, G. Biswas, V. Eswaran, Numerical prediction of heat transferin a channel with a built-in oval tube and two different shaped vortex generators, Numer. Heat Transfer Part A 41 (2002) 307–329.
[15] S. Tiwari, G. Biswas, P.L.N. Prasad, S. Basu, Numerical prediction of heat transfer in a rectangular channel with a built-in circular tube, J. Heat Transfer (ASME) 125 (2003) 413–421.
[16] H. Hornung, A.E. Perry, Some aspects of three-dimensional separation, 1: Streamsurface bifurcations, Z. Flugwiss. Weltraum Forsch. 8 (1984) 77–87.
[17] E.R.G. Eckert, E. Soehngen, Distribution of heat transfer coefficients around circular cylinders in crossflow at Reynolds numbers from 20–500, Trans. ASME 74 (1952) 343–347.
[18] W. Chun, R.F. Boehm, Calculation of forced flow and heat transfer around a cylinder in crossflow, Numer. Heat Transfer 15 (1989) 105–122.